Inorg. Chem. **2009**, *48*, 1763−1773

One- Versus Two-Electron Oxidation with Peroxomonosulfate Ion: Reactions with Iron(II), Vanadium(IV), Halide Ions, and Photoreaction with Cerium(III)

Gábor Lente,* József Kalmár, Zsuzsa Baranyai, Alíz Kun, Ildikó Kék, Dávid Bajusz, Marcell Takács, Lilla Veres, and István Fábián

University of Debrecen, Department of Inorganic and Analytical Chemistry, Debrecen 10, POB 21, Hungary, H-4010

Received August 18, 2008

The kinetics of the redox reactions of the peroxomonosulfate ion (HSO_5^-) with iron(II), vanadium(IV), cerium(III), chloride, bromide, and iodide ions were studied. Cerium(III) is only oxidized upon illumination by UV light and cerium(IV) is produced in a photoreaction with a quantum yield of 0.33 ± 0.03. Iron(II) and vanadium(IV) are most probably oxidized through one-electron transfer producing sulfate ion radicals as intermediates. The halide ions are oxidized in a formally two-electron process, which most likely includes oxygen-atom transfer. Comparison with literature data suggests that the activation entropies might be used as indicators distinguishing between heterolytic and homolytic cleavage of the peroxo bond in the redox reactions of HSO_5^-.

Introduction

Peroxomonosulfate ion (HSO_5^-), the anion of Caro's acid (H_2SO_5), is considered an inexpensive and environmentally friendly oxidant in several different applications.[1−7] In addition to high general reactivity, its main advantage over hydrogen peroxide is easier handling. It is available on a large scale in the form of a reasonably stable solid, which is commercially sold under the brand name Oxone ($2KHSO_5 \cdot KHSO_4 \cdot K_2SO_4$). The use of Oxone is without doubt more common in organic chemistry than in inorganic reactions.[8] Hydrocarbons, hydroxy and carbonyl compounds, amines, nitrogen heterocycles, sulfur, phosphorus, and halogen-containing compounds can all be oxidized using HSO_5^-.[9] There are several particularly interesting Oxone-related reactions: oxidation of alkanes in the absence of organic solvents,[10] production of singlet oxygen in its ketone-catalyzed decomposition,[11] chemiluminescence in the oxidation of carboxylic acids,[12] and autocatalysis in the oxidation of amino acids.[13]

There is ample kinetic information on various reactions of HSO_5^-.[10−24] In our recent studies on the oxidation of

* To whom correspondence should be addressed. E-mail: lenteg@delfin.unideb.hu. Tel: + 36 52 512-900/22373. Fax: + 36 52 489-667.

(1) Anipsitakis, G. P.; Dionysiou, D. D. *Environ. Sci. Technol.* **2003**, *37*, 4790–4797.
(2) Lente, G.; Espenson, J. H. *Green Chem.* **2005**, *7*, 28–34.
(3) Wong, M. K.; Chan, T. C.; Chan, W. Y.; Chan, W. K.; Vrijmoed, L. L. P.; O'Toole, D. K.; Che, C. M. *Environ. Sci. Technol.* **2006**, *40*, 625–630.
(4) Rivas, F. J.; Beltran, F. J.; Carvalho, F.; Alvarez, P. M. *Ind. Eng. Chem. Res.* **2005**, *44*, 749–758.
(5) Desai, L. V.; Malik, H. A.; Sanford, M. S. *Org. Lett.* **2006**, *8*, 1141–1144.
(6) Delcomyn, C. A.; Bushway, K. E.; Henley, M. V. *Environ. Sci. Technol.* **2006**, *40*, 2759–2764.
(7) Gandhari, R.; Maddukuri, P. P.; Vinod, T. K. *J. Chem. Educ.* **2007**, *84*, 852–854.
(8) Marcotullio, M. C.; Epifano, F.; Curini, M. *Trends Org. Chem.* **2003**, *10*, 21–34.
(9) Kennedy, R. J.; Stock, A. M. *J. Org. Chem.* **1960**, *25*, 1901–1906.
(10) Zhu, W.; Ford, W. T. *J. Org. Chem.* **1991**, *56*, 7022–7026.
(11) Lange, G.; Brauer, H. D. *J. Chem. Soc., Perkin Trans. 2* **1996**, 805–811.
(12) Wang, M.; Zhao, L.; Lin, J. M. *Luminescence* **2007**, *22*, 182–188.
(13) Kannas, R. S.; Easwaramoorthy, D.; Vijaya, K.; Ramachandran, M. S. *Int. J. Chem. Kinet.* **2008**, *40*, 44–49.
(14) Ball, D. L.; Edwards, J. O. *J. Am. Chem. Soc.* **1956**, *78*, 1125–1129.
(15) Fortnum, D. H.; Battaglia, C. J.; Cohen, S. R.; Edwards, J. O. *J. Am. Chem. Soc.* **1960**, *82*, 778–782.
(16) Montgomery, R. E. *J. Am. Chem. Soc.* **1974**, *96*, 7820–7821.
(17) Secco, F.; Venturini, M. *J. Chem. Soc., Dalton Trans.* **1976**, 1410–1414.
(18) Thompson, R. C. *Inorg. Chem.* **1981**, *20*, 3745–3748.
(19) Johnson, M. D.; Balahura, R. J. *Inorg. Chem.* **1988**, *27*, 3104–3107.
(20) Gilbert, B. C.; Stell, J. K. *J. Chem. Soc., Perkin Trans. 2* **1990**, 1281–1288.
(21) Johnson, M. D.; Nickerson, D. *Inorg. Chem.* **1992**, *31*, 3971–3974.
(22) Nolan, A. L.; Burns, R. C.; Lawarnce, G. A. *J. Chem. Soc., Dalton Trans.* **1998**, 3041–3047.
(23) Nolan, A. L.; Burns, R. C.; Lawrance, G. A. *J. Chem. Soc., Dalton Trans.* **2002**, 3065–3073.
(24) Lente, G.; Fábián, I. *Dalton Trans.* **2007**, 4268–4275.

10.1021/ic801569k CCC: $40.75
Published on Web 01/21/2009

chlorophenols,[2,24] HSO_5^- was also shown to be a useful reagent to clarify mechanistic details of catalytic oxidation reactions of hydrogen peroxide. HSO_5^- frequently acts as a two-electron oxidant in redox reactions that involve heterolytic cleavage of the peroxo bond:

$$HSO_5^- + A \rightarrow HSO_4^- + OA \quad (1)$$

In eq 1, A is a reagent with an oxygen acceptor site. In a much smaller number of reactions, HSO_5^- is proposed to be a one-electron oxidant forming the sulfate ion radical:[18,20]

$$HSO_5^- + e^- \rightarrow SO_4^{\bullet -} + OH^- \quad (2)$$

This process is analogous to the first step of Fenton-type reactions of hydrogen peroxide.

In the present work, our objective was to find a systematic way to distinguish between one- and two-electron oxidation in the reactions of HSO_5^-. We chose the simplest possible reducing agents: halide ions and some reducing metal ions. Despite the fact that the kinetic studies on some of these processes have already been published,[15,17,18] we reproduced all experiments in these cases, usually in a much wider concentration and temperature range. These experiments were designed to resolve some of the discrepancies in earlier literature data. Whenever we confirmed published rate equations, the main text will only state this fact and detailed results will be found in the Supporting Information.

In addition to the fundamental mechanistic interest in the reactions of HSO_5^-, the reductions with halide ions, and especially with Cl^-, have great practical importance as well. Oxidation of ubiquitous Cl^- to Cl_2 in water treatment technologies using Oxone may pose a serious concern regarding such applications and oxidation of Br^- to carcinogenic BrO_3^- is also a potential danger. Therefore, very reliable information is needed about this process.

Experimental Section

Materials. Potassium peroxomonosulfate stock solutions were freshly prepared every day from Oxone ($2KHSO_5 \cdot KHSO_4 \cdot K_2SO_4$, Aldrich) and standardized by iodometric titration. These acidic stock solutions were shown to be stable for at least 24 h. The known decomposition of HSO_5^- in basic medium is orders of magnitude slower than the processes we studied.[14] Perchloric and sulfuric acid was used to set the pH. In some of the experiments, the ionic strength was set with $NaClO_4$, which was prepared as described earlier.[25] In these cases, extra care was taken to make sure that the oxidant concentration is sufficiently low to avoid the precipitation of $KClO_4$ (Oxone contains K^+ ions). In other cases, H_2SO_4 or Na_2SO_4 was used to provide constant ionic strength. Halide stock solutions were prepared by weighing NaX salts and dissolving them to a known volume. All other chemicals used in this study were of analytical reagent grade and purchased from commercial sources. Doubly deionized and ultrafiltered water from a Millipore Q system was used to prepare the stock solutions and samples.

Instrumentation and Computation. UV−vis spectra and kinetic curves were recorded on PerkinElmer Lambda 25 or PerkinElmer Lambda 2S scanning and HP-8543 diode-array spectrophotometers. Fast kinetic measurements were performed with an Applied Photophysics DX-17 MV sequential stopped-flow apparatus using 1.00 cm optical path length. The dead time of the instrument was measured to be 1.09 ± 0.02 ms by published methods.[26,27] In some experiments, an Applied Photophysics PD.1 Photodiode Array accessory was used as a detector of the stopped-flow instrument. Quantitative kinetic measurements were also performed in the HP-8543 diode-array spectrophotometer using an RX-2000 Applied Photophysics Rapid Kinetics Accessory. The softwares *Scientist*[28] and *Matlab*[29] were used in the fitting procedures. A Fluorolog FL3−22 spectrofluorimeter equipped with a 450 W xenon lamp was used to detect fluorescence spectra of Ce(III).

Quantitative kinetic measurements on the photochemical reaction between HSO_5^- and Ce(III) were performed in the HP-8543 diode-array instrument using the method and general operating procedures described in earlier publications.[30,31] The solutions were kept homogeneous during the photochemical experiments using the built-in magnetic stirrer of the standard cell compartment of the HP-8543 instrument. A 3 mm stirring rod was used inside standard quartz cuvettes (optical path length: 1.000 cm). The geometry of the setup was carefully tested, and it was made sure that the stirring rod never disrupted the light beam. The light source was calibrated by both ferrioxalate actinometry[32] and reproducing observations on the known photoreaction of 2,6-dichloro-1,4-benzoquinone.[30]

Results

Halide Ions. Earlier studies of the oxidation of halide ions by HSO_5^- showed that the process was first-order with respect to both reductant and oxidant.[15,17] However, these experiments were carried out exclusively at halide excess and in acidic medium. Our own results showed that the kinetic results cannot be interpreted without considering the aqueous hydrolysis of halogens and trihalide ion formation, which are given in the following series of equilibria:

$$X_2 + H_2O = HOX + H^+ + X^- \qquad K_3 = \frac{[X^-][H^+][HOX]}{[X_2]} \quad (3)$$

$$X_2 + X^- = X_3^- \qquad K_4 = \frac{[X_3^-]}{[X_2][X^-]} \quad (4)$$

$$HOX = H^+ + OX^- \qquad K_5 = \frac{[H^+][OX^-]}{[HOX]} \quad (5)$$

The equilibrium constants for each of these three processes are known from previous literature and are summarized in Table 1.[33−38] It is also well established that these processes equilibrate on a time scale that is very short compared to

(25) Gordon, G.; Tewari, P. *J. Phys. Chem.* **1966**, *60*, 200–204.
(26) Tonomura, B.; Nakatani, H.; Ohnishi, M.; Yamaguchi-Ito, J.; Hiromi, K. *Anal. Biochem.* **1978**, *84*, 370–383.
(27) Peintler, G.; Nagy, A.; Horváth, A. K.; Körtvélyesi, T.; Nagypál, I. *Phys. Chem. Chem. Phys.* **2000**, *2*, 2575–2586.
(28) *SCIENTIST, version 2.0*; Micromath Software: Salt Lake City, UT, USA, 1995.
(29) *MatLab for Windows, version 4.2c1*, The Mathworks, Inc.: Natick, MA, USA, 1994.
(30) Lente, G.; Espenson, J. H. *J. Photochem. Photobiol., A* **2004**, *163*, 249–258.
(31) Kerezsi, I.; Lente, G.; Fábián, I. *J. Am. Chem. Soc.* **2005**, *127*, 4785–4793.
(32) Hatchard, C. G.; Parker, C. A. *Proc. R. Soc. London, Ser. A* **1956**, *235*, 518–536.

Table 1. Equilibrium and Rate Constants for the Reactions of HSO_5^- with Halide Ions

	Cl^-	Br^-	I^-
K_3 (M^2)	1.0×10^{-3} [37]	7.2×10^{-9} [38]	5.4×10^{-13} [37]
K_4 (M^{-1})	0.19 [33]	19 M^{-1} [37]	740 [37]
K_5 (M)	4.0×10^{-8} [34]	6.3×10^{-9} [35]	2.3×10^{-11} [36]
k_{HS} ($M^{-1}s^{-1}$)	$(2.06 \pm 0.03) \times 10^{-3}$	$(7.0 \pm 0.1) \times 10^{-1}$	$(1.41 \pm 0.03) \times 10^{3}$
k_S ($M^{-1}s^{-1}$)	$(3.8 \pm 0.5) \times 10^{-4}$	$(1.7 \pm 0.3) \times 10^{-1}$	$(3.0 \pm 0.2) \times 10^{2}$
pK_7	8.35 ± 0.05	8.93 ± 0.09	9.0 ± 0.1

the redox reaction with HSO_5^- studied in this work.[33−40] Therefore, for the purposes of the present study, reactions 3−5 can be assumed to be in equilibrium at all times. These reactions determine the identity of the detectable intermediates and final products over the course of the oxidation of halide ions with HSO_5^-. In the case of I^-, I_3^- is the dominating final product at reductant excess at all pH values applied in the present work. For Cl^-, Cl_2 is the dominant product at halide excess. For Br^-, however, the dominating product changes with varying pH. Figure 1 shows the UV−vis spectrum of the product in the case of Br^- at three different pH values. From these spectra, it is clear that three different dominating products appear under the three different conditions: Br_2 (together with some amount of Br_3^-) is the major product in acidic medium, HOBr in neutral, and BrO^- ion in slightly basic medium. This is in agreement with speciation calculated on the basis of literature equilibrium constants.[33−38]

The simple second-order rate equation reported in earlier works[15,17] was confirmed in this study as well (Figures S1, S2, and S3 of the Supporting Information):

$$HSO_5^- + 2X^- + 2H^+ = X_2 + HSO_4^- + H_2O$$

$$v = k_{app}[HSO_5^-][X^-] \quad (6)$$

Eq 6 gives the halogen as a final product but it is clear that this product also participates in equilibria 3−5. The pH dependence of the redox reaction was not studied in previously published works. In our experiments, perchloric acid, acetate, phosphate, and borax buffers were used in the pH region 0−10. In each case, possible buffer interferences were tested by using different absolute concentrations of the buffers setting the same pH. No dependence on the buffer concentration was detected. Figure 2 shows the dependence of k_{app} on pH for all three halide ions. The absolute values of the k_{app} rate constant varied by orders of magnitudes for different halides, therefore the y axis was normalized in Figure 2 by dividing with k_{HS} obtained in the best fit to later eq 8 to facilitate comparison of the shapes of the three curves.

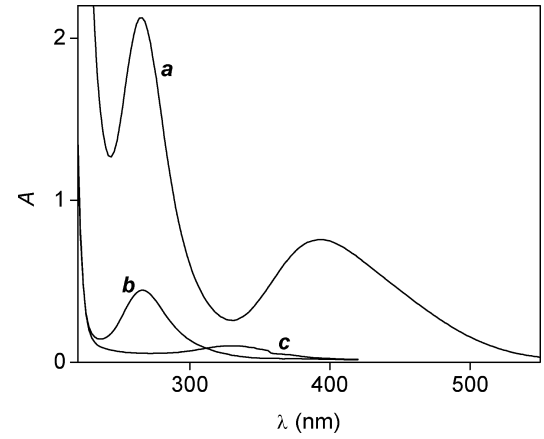

Figure 1. UV−vis spectra of the final products formed in the reaction between HSO_5^- and Br^-. $[HSO_5^-]_0 = 1.0$ mM; $[Br^-]_0 = 2.1$ mM (***a***), 10 mM (***b***,***c***); pH = 0.8 (***a***), 6.3 (***b***), 9.2 (***c***); path length, 1.000 cm; $T = 25.0$ °C. $\lambda_{max} = 262$ nm (HOBr); $\lambda_{max} = 266$ nm (Br_3^-); $\lambda_{max} = 332$ nm (OBr^-); $\lambda_{max} = 394$ nm (Br_2).[39]

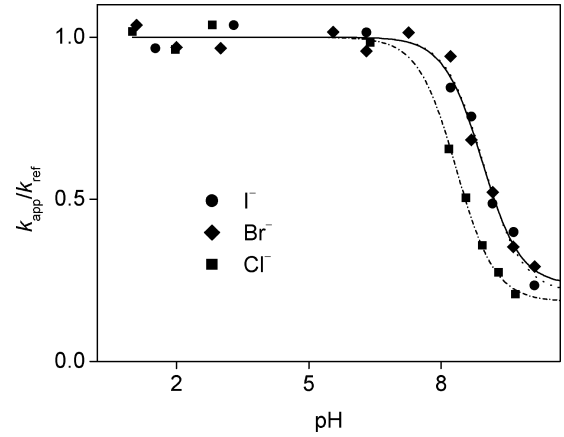

Figure 2. pH dependencies of the normalized apparent second-order rate constants determined in the reactions between HSO_5^- and various halide ions. Medium: 0.10 M $NaClO_4$ (Br^-, I^-), 1.0 M $NaClO_4$ (Cl^-); $T = 25.0$ °C; $k_{ref} = 2.06 \times 10^{-3}$ $M^{-1}s^{-1}$ (Cl^-), 7.0×10^{-1} $M^{-1}s^{-1}$ (Br^-), 1.41×10^3 $M^{-1}s^{-1}$ (I^-).

The apparent second-order rate constant k_{app} was independent of pH in the acidic region but dropped sharply in the pH region 7−10. The pH dependence is interpreted by the acid dissociation of HSO_5^-:

$$HSO_5^- = H^+ + SO_5^{2-} \qquad K_7 = \frac{[H^+][SO_5^{2-}]}{[HSO_5^-]} \quad (7)$$

The following equation could be used to fit the rate constants for all three halides:

$$k_{app} = \frac{k_{HS}[H^+] + k_S K_7}{[H^+] + K_7} \quad (8)$$

The fitted values of constant K_7 are also shown in Table 1. The literature values of pK_7 are 9.4[14] and 9.3.[41] Our values are slightly lower but this is not unexpected as the ionic strength (0.10 M) we used in the I^- and Br^- study is higher than that in previous works.[14,41] The value of pK_7 in the reaction with Cl^- is even lower, again due to the higher ionic

(33) Sherill, M. S.; Izard, E. F. *J. Am. Chem. Soc.* **1931**, *53*, 1667–1674.
(34) Adam, L. C.; Fábián, I.; Suzuki, K.; Gordon, G. *Inorg. Chem.* **1992**, *31*, 3534–3541.
(35) Gerritsen, C. M.; Gazda, M.; Margerum, D. W. *Inorg. Chem.* **1993**, *32*, 5739–5748.
(36) Lengyel, I.; Epstein, I.; Kustin, K. *Inorg. Chem.* **1993**, *32*, 5880–5882, and references therein.
(37) Lengyel, I.; Li, J.; Kustin, K.; Epstein, I. *J. Am. Chem. Soc.* **1996**, *118*, 3708–3719, and references therein.
(38) Tóth, Z.; Fábián, I. *Inorg. Chem.* **2000**, *39*, 4608–4614, and references therein.
(39) Tóth, Z.; Fábián, I. *Inorg. Chem.* **2004**, *43*, 2717–2723, and references therein.
(40) Wang, T.; Margerum, D. W. *Inorg. Chem.* **1994**, *33*, 1050–1055.
(41) Goodman, J. F.; Robson, P. *J. Chem. Soc.* **1963**, 2871–2875.

Table 2. Activation Parameters in Some Redox Reactions of HSO_5^-

reductant	$\Delta H^{\ddagger}$ (kJ/mol)	$\Delta S^{\ddagger}$ (J/mol/K)	$k_{25\ °C}$ ($M^{-1}s^{-1}$)	ref
Cl^-	58.9 ± 0.5	−100 ± 2	2.1×10^{-3}	[a]
	59	−73	1.8×10^{-3}	15
Br^-	44.8 ± 1.6	−97 ± 5	7.0×10^{-1}	[a]
	42	−104	1.0×10^{0}	15
I^-	27.7 ± 0.7	−91 ± 2	1.4×10^{3}	[a] I^- excess
	29.4 ± 0.5	−86 ± 2	1.4×10^{3}	[a] HSO_5^- excess
	31	−79	1.7×10^{3}	17
I_2	50.8 ± 0.5	−90 ± 2	1.2×10^{-1}	[a]
VO^{2+}	59 ± 2	−27 ± 7	1.4×10^{1}	[a]
	54	−46	1.3×10^{1}	18
	53.7 ± 0.04	−44 ± 1	---	[b]
Fe^{2+}	38.5 ± 0.9	−34 ± 3	3.7×10^{4}	[a]
$(CH_3)_2S$	51.3	−87	1.3×10^{-1}	60
$(C_2H_5)_2S$	40.7	−120	2.9×10^{-1}	60
HSO_3^-	25.7	−88	4.9×10^{3}	61
N_3^-	49	−84	6.6×10^{-1}	62
HN_3	61	−130	2.0×10^{-5}	62
$C_6H_5COSC_6H_5$ [c]	54	−96	6.8×10^{-3}	63

[a] This work. [b] Data from reference 18 reinterpreted in this work. [c] The reactions of 11 more, differently substituted thioesters have very similar entropies of activation (ref 63)

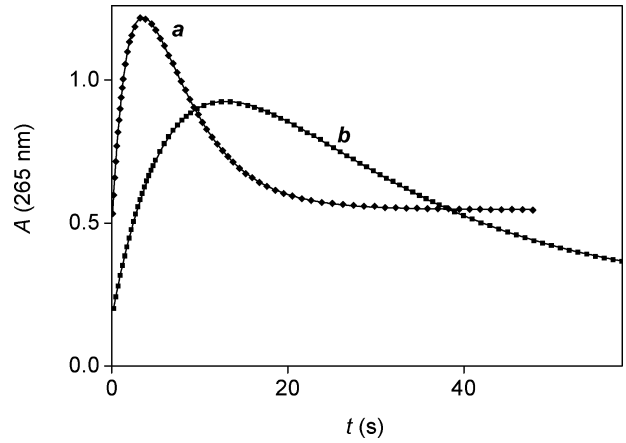

Figure 3. Kinetic traces in the reaction between HSO_5^- and Br^-. Markers: measured points (only about 10% of measured points shown for clarity). Lines: fitted double exponential curves. $[HSO_5^-]_0 = 64$ mM (***a***), 18 mM (***b***); $[Br^-]_0 = 2.0$ mM; pH 0.40; path length, 1.00 cm; $T = 25.0$ °C; medium, 0.40 M H_2SO_4.

strength (1.0 M). The primary reason for the higher ionic strength was that high Cl^- concentrations had to be maintained in acidic media to follow the absorption of the strongly absorbing Cl_3^- because Cl_2 had too small molar absorptivities for reliable detection. Activation parameters were determined for the HSO_5^--oxidation pathways k_{HS} (Figure S4 in the Supporting Information) in a series of measurements in strongly acidic medium ($[H^+] \gg K_7$). These values are listed in Table 2 along with activation parameters for other reactions.

The ionic strength dependence of the kinetics of the oxidation of Br^- (Figure S5 in the Supporting Information) could be interpreted as a kinetic salt effect based on the Debye−Hückel theory[42] acceptably:

$$\log k = \log k^{\circ} + 2Az_1z_2\sqrt{I} \qquad (9)$$

where $A = 0.509\ M^{-1/2}$ is the Debye−Hückel parameter.[42] Fitting the points measured at relatively low ionic strength ($I \leq 0.04$ M) to eq 9 gave the parameters $z_1z_2 = 1.13 \pm 0.13$ and $\log k^{\circ} = -0.40 \pm 0.04$, which further confirms that the rate-determining step is the direct interaction of the mononegative HSO_5^- with mononegative halide ions.

Experiments were also carried out at oxidant excess. Similar data have not been published thus far. These conditions are fairly important for possible applications in water treatment technology where the oxidant may typically be present in excess over the halide ions. Under these conditions, the identities of the final products are different from those at reductant excess. Br_2 and I_2 are long-lived intermediates when Br^- and I^- are oxidized, and the final products, BrO_3^- and IO_3^- ions, are produced in kinetically separate steps. In the oxidation of Cl^-, HOCl is the final product.

The change in absorbance was monitored at several wavelengths for all reactions. In the case of Br^-, 395 nm was used for monitoring the buildup of Br_2 (Figure S6 in the Supporting Information). These curves were simple exponential traces, the confirmed rate equation and rate constant was practically the same as the one detected at halide ion excess (Figure S7 in the Supporting Information). Because of the high concentration of potassium ion due to the large Oxone excess, perchlorate salts could not be used to set the ionic strength. The value of k_{HS} was 1.75 ± 0.05 $M^{-1}s^{-1}$ in 0.40 M H_2SO_4, which compares well with the value 1.7 $M^{-1}s^{-1}$ determined in 1.0 M $NaClO_4$ at Br^- excess. When the process was monitored at 265 nm, as shown in Figure 3 and Figure S8 in the Supporting Information, the formation of an intermediate was evident. This may be surprising at first sight. However, the wavelength is primarily sensitive to Br_3^- ($\varepsilon = 4.09 \times 10^4\ M^{-1}cm^{-1}$)[38] and HSO_5^- also contributes somewhat to the absorbance measured at this wavelength (the concentration of HSO_5^- is practically constant because it is in large excess). Equilibrium 4 ensures that some amount of Br_3^- is present in the mixture, whereas reactant Br^- and product Br_2 are simultaneously present. Reaction 4 equilibrates much faster than the studied redox process.[38] The conditions are such that the concentration of Br_3^- ion is negligibly small compared to the sum of the concentrations of Br^- and Br_2.

$$[Br^-] + [Br_2] \gg [Br_3^-] \qquad (10)$$

Therefore, the concentration of Br_3^- can be neglected when writing mass balances, and this simplifies mathematical deductions. However, Br_3^- is still detected at the appropriate wavelength because it has an exceptionally large molar absorptivity. As shown by the measurements at 395 nm, Br_2 is produced in a pseudo-first-order process, therefore the loss of Br^- should also be pseudo-first-order:

$$[Br^-] = [Br^-]_0 e^{-kt} \text{ and } [Br_2] = [Br^-]_0(1 - e^{-kt}) \qquad (11)$$

As reaction 4 equilibrates much faster than the redox reaction proceeds, the concentration of Br_3^- can be calculated in a straightforward way:

(42) Atkins, P. W. *Physical Chemistry*, 6th ed.; Oxford University Press: Oxford, 1998; p 836.

$$[Br_3^-] = K_{4,Br}[Br^-][Br_2] = K_{4,Br}[Br^-]_0 e^{-kt}(1 - e^{-kt})$$
$$= -K_{4,Br}[Br^-]_0 e^{-2kt} + K_{4,Br}[Br^-]_0 e^{-kt} \quad (12)$$

This function might be called an apparent double exponential function because its two time constants are not independent; the first is exactly twice as high the second. Eq 12, allowing for the absorbance contribution of excess HSO_5^-, described the experimentally detected curves very well as shown by the solid lines in Figure 3.

When I^- was oxidized, the chemical background of our observations was essentially the same as that in the Br^- reaction. At 465 nm, a steady increase in the concentration of I_2 was detected (Figure S9 in the Supporting Information). Curves detected at 365 nm are shown in Figure 4 and in Figure S10 in the Supporting Information. This wavelength is exclusively selective for I_3^-. The value of the formation constant of I_3^- (Table 1) is such that a simplification analogous to eq 10 cannot be used, which makes the mathematical description more complicated. As shown in the Supporting Information, the following implicit function gives the concentration of I^- as a function of time:

$$\frac{2 + K_{4,I}[I^-]_0}{2} \ln \frac{[I^-]}{[I^-]_0} - \frac{2 + 3K_{4,I}[I^-]_0}{6} \ln \frac{2 + 3K_{4,I}[I^-]}{2 + 3K_{4,I}[I^-]_0} +$$
$$K_{4,I} \frac{[I^-]_0 - [I^-]}{2 + 3K_{4,I}[I^-]} = -2k_{HS,I}[HSO_5^-]t \quad (13)$$

When the concentration of I^- is calculated from eq 13, the concentrations of the other two species can be calculated by straightforward algebra:

$$[I_2] = \frac{[I^-]_0 - [I^-]}{2 + 3K_{4,I}[I^-]} \quad (14)$$

$$[I_3^-] = K_{4,I}[I^-] \frac{[I^-]_0 - [I^-]}{2 + 3K_{4,I}[I^-]} \quad (15)$$

The implicit function and eqs 14−15 gave a reasonably good interpretation of the experimental kinetic curves as shown by the fitted curves in Figure 4. Curves measured at 365 nm were also used in a temperature-dependent study (Figure S11 in the Supporting Information). As expected, the activation parameters agreed very well with the ones determined at reductant excess.

Another difference between the reactions of Br^- and I^- was that the further oxidation of I_2 could be studied without problems. In the Br^- system, evidence of further oxidation of Br_2 was also obtained but it was much slower and quantitative measurements were not possible because the process was strongly coupled with the disproportionation of HSO_5^-, which produces O_2, and spectrophotometric detection of the reaction was unavoidably corrupted by bubble formation in the cell. Representative kinetic traces for the oxidation of I_2 are shown in Figure 5. The inset shows that a two-term rate equation was confirmed for this process:

$$2I_2 + 5HSO_5^- + H_2O = 2IO_3^- + 5HSO_4^- + 2H^+$$
$$v = k_{16a}[I_2] + k_{16b}[I_2][HSO_5^-] \quad (16)$$

The parameters $k_{16a} = (4.9 \pm 0.9) \times 10^{-4}\ s^{-1}$ and $k_{16b} = 0.117 \pm 0.002\ M^{-1}s^{-1}$ were resolved in the linear fit of the pseudo-first-order rate constant as a function of $[HSO_5^-]$. A temperature-dependent study of k_{16b} (Figure S12 in the Supporting Information) yielded the activation parameters given in Table 2.

The oxidation of Cl^- at HSO_5^- excess was quite different. First of all, the formation constant of Cl_3^- is low enough that equilibrium 4 did not influence the measurements in any way. However, the final product was not the appropriate halogen, but HOCl in this case. In addition, Cl_2 was detected as an intermediate in this process. This is a consequence of equilibrium 3: while Cl^- and HOCl are present simultaneously, some Cl_2 also forms. The equilibrium constant of reaction 3 is such that the amount of Cl_2 is significant compared to the concentrations of reactants and products.

The combination of equilibrium 3 and irreversible redox reaction 6 gave a set of kinetic equations that could be solved analytically with a strategy similar to that used with I^-:

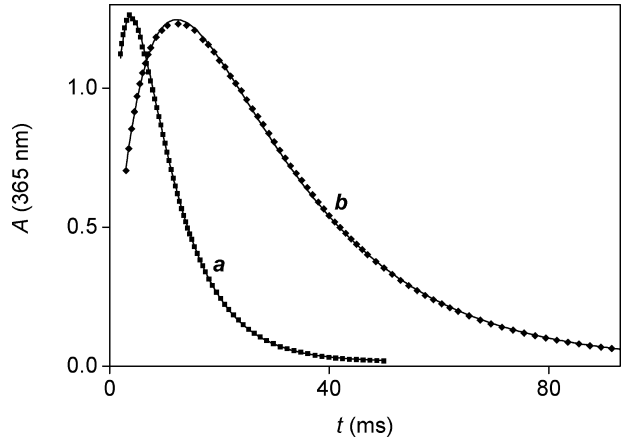

Figure 4. Kinetic traces in the reaction between HSO_5^- and I^-. Markers: measured points (only about 10% of measured points shown for clarity). Lines: best fit to eqs 13−15. $[HSO_5^-]_0 = 64$ mM (***a***), 18 mM (***b***); $[I^-]_0 = 1.0$ mM; pH 0.40; path length, 1.00 cm; $T = 25.0$ °C; medium, 0.40 M H_2SO_4.

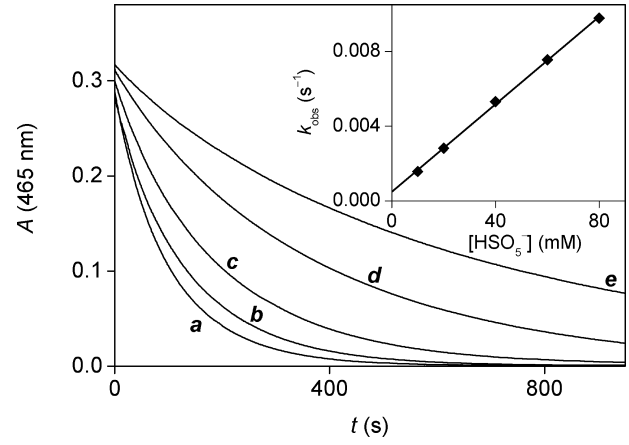

Figure 5. Kinetic traces in the reaction between HSO_5^- ion and I_2. Inset: dependence of the pseudo first-order rate constants on HSO_5^- concentration. $[HSO_5^-]_0 = 80$ mM (***a***), 60 mM (***b***), 40 mM (***c***), 20 mM (***d***), 10 mM (***e***); $[I_2]_0 = 0.50$ mM; pH 0.40; path length, 1.000 cm; $T = 25.0$ °C; medium, 0.40 M H_2SO_4.

$$(1 + [H^+][Cl^-]_0/K_{3,Cl}) \ln \frac{[Cl^-]}{[Cl^-]_0} - \frac{1 + 2[H^+][Cl^-]_0/K_{3,Cl}}{2} \ln \frac{1 + 2[H^+][Cl^-]/K_{3,Cl}}{1 + 2[H^+][Cl^-]_0/K_{3,Cl}} + [H^+]\frac{[Cl^-]_0 - [Cl^-]}{K_{3,Cl} + 2[H^+][Cl^-]} = -k_{HS,Cl}[HSO_5^-]t \quad (17)$$

After the Cl^- concentration is obtained from eq 17, the concentrations of Cl_2 and HOCl can be calculated by straightforward equations:

$$[HOCl] = \frac{[Cl^-]_0 - [Cl^-]}{1 + 2[H^+][Cl^-]/K_{3,Cl}} \quad (18)$$

$$[Cl_2] = [H^+][Cl^-]/K_{3,Cl}\frac{[Cl^-]_0 - [Cl^-]}{1 + 2[H^+][Cl^-]/K_{3,Cl}} \quad (19)$$

Formulas 17−19 were sufficient to interpret the kinetic traces (fitted curve in Figure S13 in the Supporting Information). This observation implies that the direct reaction of Cl_2 with HSO_5^- does not contribute detectably to the measured rate.

Vanadium(IV). In an earlier work, a manual mixing technique was used to explore the kinetics of the redox reaction between V(IV) and HSO_5^-.[18] This severely limited the concentration and temperature range of the experiments as the process is quite fast; it is usually complete in a few seconds. Our kinetic studies were carried out by the stopped-flow method. The rate equation and stoichiometry reported in the earlier work[18] were confirmed in our experiments as well (Figures S14−S18 in the Supporting Information):

$$2VO^{2+} + HSO_5^- + H_2O = 2VO_2^+ + HSO_4^- + 2H^+$$

$$v = [VO^{2+}][HSO_5^-]\left(k_{20a} + \frac{k_{20b}}{[H^+]}\right) \quad (20)$$

The parameters $k_{20a} = 14.4 \pm 0.4\ M^{-1}s^{-1}$ and $k_{20b} = (1.3 \pm 0.2) \times 10^{-1}\ s^{-1}$ were calculated. Our measurements were done both with HSO_5^- and V(IV) in excess. At reductant excess, the pseudo-first-order rate constant k_{obs} is related to k_{20a} and k_{20b} as follows:

$$k_{obs} = [VO^{2+}](k_{20a} + k_{20b}/[H^+]) \quad (21)$$

At oxidant excess, however, the 2:1 stoichiometry of the reaction results in a slightly different formula:

$$k_{obs} = 2[HSO_5^-](k_{20a} + k_{20b}/[H^+]) \quad (22)$$

A similar relationship will be important in the study of the Fe(II) system as well. Activation parameters for k_{20a} path were determined (Figure S19 in the Supporting Information) and are shown in Table 2. The activation parameters are somewhat different form the values published in the earlier work.[18] As shown in Figure S19 in the Supporting Information, the agreement between the rate constants is excellent at room temperature but gets worse as the temperature decreases. Higher temperatures were not included in the earlier study because of experimental limitations. We also noted a small numerical error in the reported activation parameters, so Table 2 also includes the values we calculated in the re-evaluation of the published data.[18]

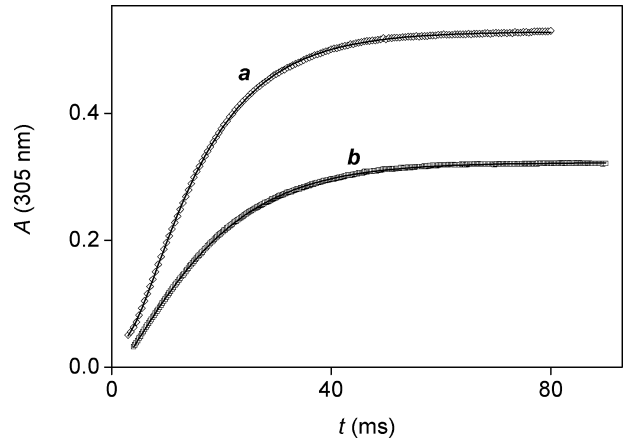

Figure 6. Kinetic traces in the reaction between HSO_5^- and Fe(II). Markers, measured points (only about 10% of measured points shown for clarity); lines, best fit to eqs 27−28. $[HSO_5^-]_0 = 2.20$ mM (***a***), 0.092 mM (***b***); $[Fe(II)]_0 = 0.27$ mM (***a***), 2.72 mM (***b***); pH 0.80; path length, 1.00 cm; $T = 25.0$ °C; medium, 0.10 M H_2SO_4.

Iron(II). There is a single reference known to us that gives the second-order rate constant of the reaction between aqueous Fe(II) and HSO_5^-.[20] Unfortunately, no kinetic details or method specification is given in that work. On the basis of the reported rate constant, we expected simple kinetics for the redox reaction between Fe(II) and HSO_5^-. In contrast, the measured kinetic traces (examples are given in Figure 6) clearly reflected a more complicated two-step process.

The influence of sulfate ion is very important in this system. Unfortunately, its presence is unavoidable. Even if Oxone were completely purified of its sulfate ion content, the redox reaction itself produces significant amounts of sulfate ion from HSO_5^- by the end of the process. Sulfate ion is known to complex the other product of the process, Fe(III):[43,44]

$$Fe^{3+} + SO_4^{2-} = FeSO_4^+ \qquad K_{23} = \frac{[FeSO_4^+]}{[Fe^{3+}][SO_4^{2-}]} \quad (23)$$

To keep the concentration of sulfate ion constant, experiments were carried out in sulfuric acid. In this medium, the protonation of SO_4^{2-} has to be taken into account.

$$HSO_4^- = H^+ + SO_4^{2-} \qquad K_{24} = \frac{[H^+][SO_4^{2-}]}{[HSO_4^-]} \quad (24)$$

The values $K_{23} = 115\ M^{-1}$ and $K_{24} = 0.087$ M are available from the literature.[43] On the basis of literature data, reaction 23 is expected to equilibrate with a relaxation time of 7.5 ms in 0.10 M H_2SO_4,[43] which is similar to the time scale of the redox reaction.

As the kinetics of the reaction showed unexpected features, the stoichiometry was tested very carefully. The results of

(43) Lente, G.; Fábián, I. *Inorg. Chem.* **2002**, *41*, 1306–1314.
(44) Kormányos, B.; Peintler, G.; Nagy, A.; Nagypál, I. *Int. J. Chem. Kinet.* **2008**, *40*, 114–124.

two photometric titration are shown in Figure 7. Both of these titrations were consistent with a 2:1 Fe^{2+}/HSO_5^- stoichiometric ratio. The UV−vis spectrum of the final product of the reaction was also shown to be identical to the spectrum of Fe(III) in sulfuric acid (Figure S20 in the Supporting Information). These observations clearly prove that Fe(III) and sulfate ions are the products of the redox reaction.

Time-resolved spectra measured during the course of the redox process showed no evidence of an absorbing intermediate (Figure S21 in the Supporting Information). Straightforward kinetic studies were somewhat hindered by the fact that the process was quite fast and it was impossible to use either of the reagents in very high excess (e.g., 100-fold excess). Therefore, most of the measurements were carried out under conditions where neither of the reagents were in very high excess. The last parts of the measured kinetic traces (from 50 to 80% conversion depending of the stoichiometric ratio of the reactants) could be fitted quite well to exponential functions. During this last part, the concentration of the excess reagent can be regarded as constant (Δ), which is given as $\Delta = [Fe(II)]_0 - {}^1/_2[HSO_5^-]_0$ for Fe(II) excess and $\Delta = [HSO_5^-]_0 - 2[Fe(II)]_0$ for oxidant excess. The fitted pseudo-first-order rate constant is fully analogous to k_{obs} used in earlier systems. As noted at the V(IV) study, it should be kept in mind that k_{obs} equals k[Fe(II)] at Fe(II) excess, whereas k_{obs} gives $2k[HSO_5^-]$ at HSO_5^- excess. Figure 8 shows k_{obs} or ${}^1/_2k_{obs}$ as a function of Δ. It is seen that a linear relationship is maintained throughout the entire concentration range studied. The good exponential fits of the final parts of the curves and the linear dependence shown in Figure 8 are fully consistent with a process that is first-order with respect to both of its reagents.

When about 20-fold excess of a reagent was used over the other, its concentration could be considered constant during the entire course of the reaction. In these experiments, double exponential curves were observed:

$$A = A_1 e^{-k_{obs1}t} + A_2 e^{-k_{obs2}t} + E \quad (25)$$

In some exceptional cases, the two time constants of the double exponential curve apparently coincided. This gives

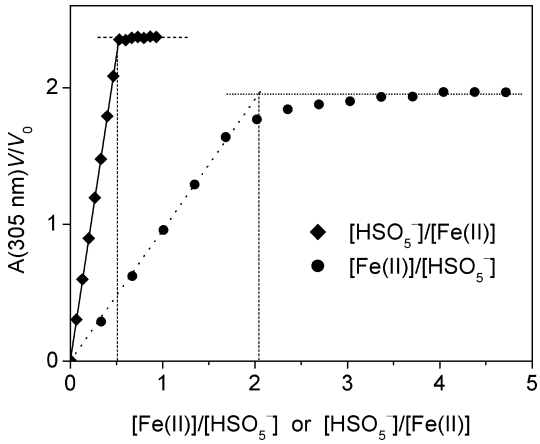

Figure 7. Spectrophotometric titrations in the reaction between HSO_5^- and Fe(II). Titration 1 (diamonds), $[Fe(II)]_0 = 1.00$ mM; $[HSO_5^-]_{titr} = 1.50$ mM; titration 2 (circles), $[HSO_5^-]_0 = 1.50$ mM; $[Fe(II)]_{titr} = 3.00$ mM; common parameters, $V_0 = 2.00$ cm^3; pH 2.0; path length, 1.000 cm; $T = 25.0$ °C.

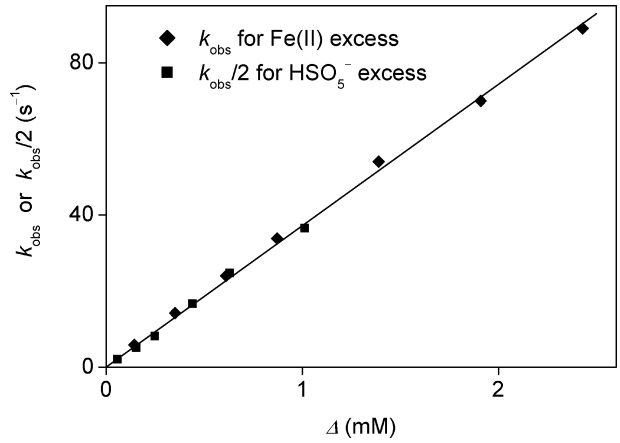

Figure 8. Concentration dependence of pseudo-first-order rate constants fitted for the last parts of the kinetic curves in the reaction between HSO_5^- and Fe(II); pH 0.80; $T = 25.0$ °C; medium, 0.10 M H_2SO_4.

rise to a new algebraic form for concentrations in the two-step process and the absorbance could be fitted to the following equation:[45]

$$A = (A_1 + A_2 t)e^{-k_{obs12}t} + E \quad (26)$$

At first, these findings may be surprising because a double exponential curve implies a detectable intermediate, in contrast with the conclusion drawn from the time-resolved spectra.

The observations can be interpreted by a straightforward model:

$$2Fe^{2+} + HSO_5^- + H^+ \rightarrow 2Fe^{3+} + SO_4^{2-} + H_2O$$
$$v = k_{27}[Fe^{2+}][HSO_5^-] \quad (27)$$

$$Fe^{3+} + SO_4^{2-} \rightleftharpoons FeSO_4^+$$
$$v = k_{28}[Fe^{3+}][SO_4^{2-}] - k_{-28}[FeSO_4^+] \quad (28)$$

Parameters k_{28} and k_{-28} are pH-dependent apparent rate constants, the pH dependence of which was explored earlier.[43,44] When one of the reagents is used in large excess, the concentration of this reagent is constant and the mathematical description can be simplified to two consecutive pseudo-first-order processes, which gives a double exponential curve. A double exponential absorbance−time curve does not imply that the reaction with the faster rate constant actually occurs first in the sequence.[45] In fact, we concluded that in our special case the fast rate constant usually characterizes the second process (eq 28), whereas the slow rate constant corresponds to the first process (eq 27).[45] This is clearly evidenced by the fact that the fast observed rate constant is in good agreement with the pseudo-first-order rate constants calculated from literature data for reaction 28 (Table S1 in the Supporting Information).[43,44] This explanation also makes it clear why no absorbing intermediate was identified despite the fact that Fe(III) does absorb in this spectral region. The molar absorptivities of the Fe(III) hexaqua complex are lower than those of

(45) Espenson, J. H. In *Chemical Kinetics and Reaction Mechanisms*, 2nd ed.; McGraw-Hill: New York, 1995.

$Fe(SO_4)^+$,[43] and Fe(III) is only produced in relatively low concentrations, so its absorbance contribution remains negligible. It is also clear why the approach with fitting the final parts of the curves was successful: after some initial time, reaction 27 becomes fully rate-limiting. From the fit shown in Figure 8, $k_{27} = (3.72 \pm 0.03) \times 10^4\ M^{-1}s^{-1}$ was determined.

A final test of the proposed kinetic model is the integration of differential equations defined by the chemical model. The analytical solution for this two-step scheme under second-order conditions (i.e., none of the reagents is in large excess) is possible but does not yield a closed form suitable for fitting.[46] Numerical integration, however, can be used in a straightforward way to fit the model to the experimental curves. This procedure, which was used in a fully analogous way in our earlier studies,[43,47] showed that these two consecutive reactions interpret the kinetic traces well. Fitted curves are shown in Figure 6 and residuals are shown in Figure S22 in the Supporting Information.

Another set of calculations were performed including the following step instead of eq 27:

$$2Fe^{2+} + HSO_5^- + H^+ \rightarrow Fe^{3+} + Fe(SO_4)^+ + H_2O \quad (29)$$

The model given in eqs 28 and 29, which is primarily different from eqs 27 and 28 in the stoichiometry of the first step, gave a somewhat worse but still acceptable fit to the measured kinetic traces. Both fits are actually shown in Figure 6 but they are indistinguishably close to each other. The residuals of the two sample traces with the two different fits (Figure S22 in the Supporting Information) showed that the model with eqs 27 and 28 gave a significantly better fit than eqs 28 and 29, although the difference was not highly significant. On the basis of these results, the first model seems to be more likely but the second model cannot be excluded either.

The influence of pH on the redox process was studied by changing the concentration of H_2SO_4 and maintaining the ionic strength by adding Na_2SO_4 when needed. The pseudo-first-order rate constants fitted to the last parts of the kinetic curves did not depend on the pH, that is the rate of reaction 27 is pH-independent. However, the kinetic curves themselves did depend on the pH because the kinetics of the complexation step, eq 28, is pH-dependent. Activation parameters for reaction k_{27} were also determined (Figure S23 in the Supporting Information) and are listed in Table 2.

Cerium(III). When a $CeCl_3$ solution was mixed with oxone solution in the dark, no decrease in the concentration of Ce(III) could be detected, only the slow oxidation of Cl^- was observed in agreement with our direct study on the $Cl^- - HSO_5^-$ system. However, when the same reaction was studied in a diode array spectrophotometer, quite significant spectral changes were observed (Figure 9). The lamp of the spectrophotometer induces a photoreaction in the system. This effect is well-known as a source of error in diode array spectrophotometric studies[47,48] and can be used for photochemical studies.[30,31,47]

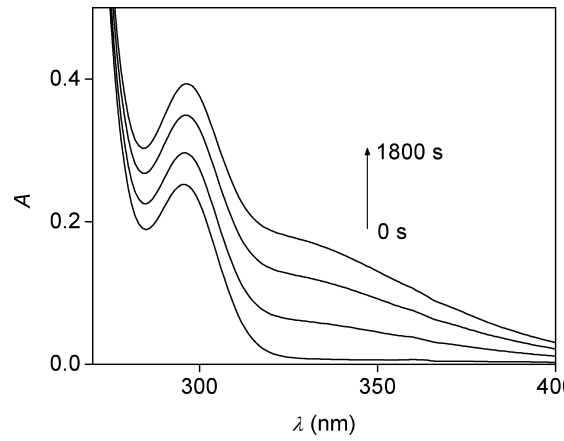

Figure 9. Time-resolved UV−vis spectra in the photochemical reaction between HSO_5^- and Ce(III); $[Ce^{3+}] = 5.1$ mM; $[HSO_5^-] = 0.56$ mM; pH 0.30; path length, 1.000 cm; $T = 25.0$ °C; medium, 0.50 M H_2SO_4.

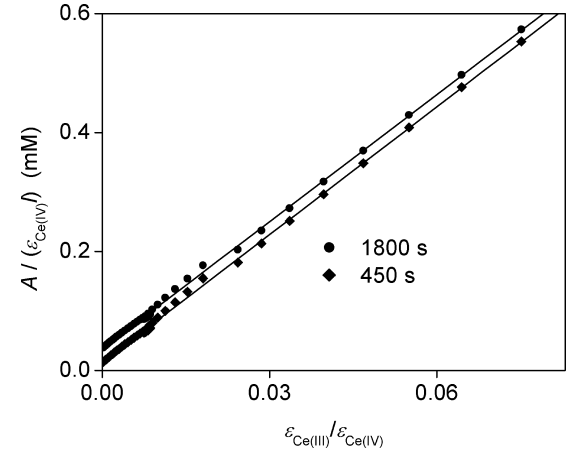

Figure 10. Analysis of time-resolved UV−vis spectra in the photochemical reaction between HSO_5^- and Ce(III) according to eq 31.

The molar UV−vis spectra of Ce(III), Ce(IV), and HSO_5^- (Figure S24 in the Supporting Information) were recorded in a series of measurements with different concentrations to make sure that molar absorptivities are known with high accuracy at each wavelength. HSO_5^- does not absorb significantly above 250 nm. Absorbance readings above 266 nm (Figure 9) were analyzed assuming that they correspond to the sum of absorbances of Ce(III) and Ce(IV). Beer's law for two absorbing species takes the following form:

$$A^\lambda = \varepsilon^\lambda_{Ce(IV)}[Ce(IV)]l + \varepsilon^\lambda_{Ce(III)}[Ce(III)]l \quad (30)$$

A rearrangement of this equations gives:

$$\frac{A^\lambda}{\varepsilon^\lambda_{Ce(IV)}l} = [Ce(IV)] + [Ce(III)]\frac{\varepsilon^\lambda_{Ce(III)}}{\varepsilon^\lambda_{Ce(IV)}} \quad (31)$$

A plot of $A^\lambda/(\varepsilon^\lambda_{Ce(IV)}l)$ against $\varepsilon^\lambda_{Ce(III)}/\varepsilon^\lambda_{Ce(IV)}$ should therefore give a straight line at any reaction time. This plot is shown in Figure 10 at two reaction times. The linearity of the plot proves that the spectral changes are caused by the conversion of Ce(III) to Ce(IV):

(46) Anderson, R. L.; Nohr, R. S.; Spreer, L. O. *J. Chem. Educ.* **1975**, *52*, 437–438.
(47) Galajda, M.; Lente, G.; Fábián, I. *J. Am. Chem. Soc.* **2007**, *129*, 7738–7739.
(48) Stanbury, D. M.; Figlar, J. N. *Coord. Chem. Rev.* **1999**, *187*, 223–232.

$$2Ce^{3+} + HSO_5^- + H^+ \rightarrow 2Ce^{4+} + SO_4^{2-} + H_2O \quad (32)$$

A calibration of the lamps of the spectrophotometer[30,31] also allowed the determination of the quantum yield of the photoreaction, which was calculated to be 0.33 ± 0.03 for the formation of Ce(IV). A series of kinetic experiments were also carried out by introducing dark periods into the course of illumination. Kinetic curves with four different dark-period lengths are shown in Figure 11. The illumination ratio[31] in these experiments is defined as the illumination time divided by total time elapsed. The inset in Figure 11 shows that the initial rate of the reaction is directly proportional to the illumination ratio.

Interestingly, the fluorescence of Ce(III)[49] was visible to the naked eye during the photochemical experiments in the spectrophotometer (Photo S1 in the Supporting Information). Quantitative measurements showed that the fluorescence intensity of Ce(III) was not influenced by the presence of HSO_5^- under conditions when the photoreaction proceeds (Figure S25 in the Supporting Information).

Discussion

The reactions of the halide ions with HSO_5^- seem to be two-electron processes, most likely a straightforward oxygen-atom transfer followed by or coupled to a proton transfer. The full rate equation given in eq 7 can be interpreted by two parallel pathways:

$$X^- + HSO_5^- \rightarrow OX^- \rightarrow + HSO_4^- \qquad v = k_{HS}[X^-][HSO_5^-] \quad (33)$$

$$X^- + SO_5^{2-} \rightarrow OX^- + SO_4^{2-} \qquad v = k_S[X^-][SO_5^{2-}] \quad (34)$$

In fact, these reactions and the coupled fast equilibria in eqs 3−5 are sufficient to interpret all of the findings at oxidant excess as well. Most notably, there was no need to assume that I_3^-, Br_3^-, or Cl_2 are directly oxidized by HSO_5^- under oxidant excess. If these possible pathways were to contribute significantly to the oxidation rate, the formulas given in eqs 12, 13, and 17 could not have been used successfully to describe the experimentally measured curves.

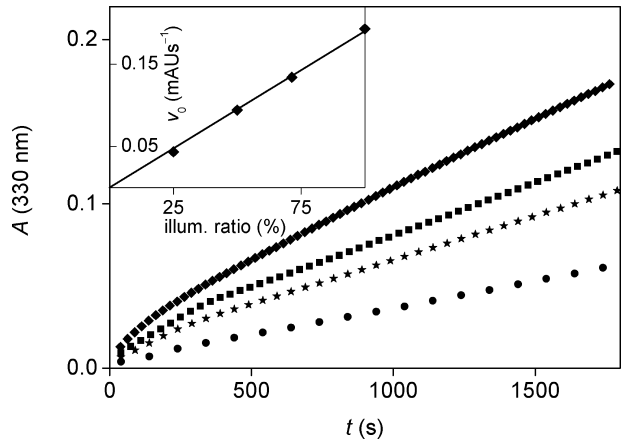

Figure 11. Kinetic traces in the photochemical reaction between HSO_5^- and Ce(III) at different illumination ratios; inset, initial rates as a function of illumination ratio; $[Ce^{3+}] = 5.1$ mM; $[HSO_5^-] = 0.56$ mM; pH 0.30; path length, 1.000 cm; $T = 25.0$ °C; medium, 0.50 M H_2SO_4.

For the oxidation of I_2 to IO_3^-, a simple series of reactions can be envisaged:

$$I_2 + HSO_5^- \rightarrow I_2O + HSO_4^- \qquad v = k_{35}[I_2][HSO_5^-] \quad (35)$$

$$I_2O + H_2O \rightarrow 2HOI \quad (36)$$

$$HOI + HSO_5^- \rightarrow HIO_2 + HSO_4^- \quad (37)$$

$$HIO_2 + HSO_5^- \rightarrow IO_3^- + H^+ + HSO_4^- \quad (38)$$

If reaction 35 is rate limiting in this sequence and the others are fast, this series interprets the k_{16b} pathway of the oxidation with $k_{16b} = k_{35}$. Reactions 36−38 occur after the rate-determining step and they are only included to give a chemically feasible way to account for the stoichiometry. Various oxyiodine species may also react with each other, but these steps only occur after the rate-determining process and do not influence the observed kinetics. The other pathway, k_{16a}, which is independent of oxidant concentration, is interpreted by the hydrolysis of I_2 (the forward process of equilibrium 3) being rate determining. The fitted value of k_{16a} is consistent with independent data on the kinetics of I_2 hydrolysis,[36] and it is already known that I^- (one of the products of iodine hydrolysis) reacts with HSO_5^- quite rapidly.

In the Fe(II) reaction, both one- and two-electron oxidations seem possible at first sight. The two-electron oxidation route should involve aqueous Fe(IV), that is ferryl ion (FeO^{2+}) and could be an oxygen-atom transfer in the rate-limiting step. Ferryl ion was identified in earlier studies.[50,51] However, we think only the one-electron pathway is viable here. If FeO^{2+} were involved in the process, there should be a second detectable intermediate at oxidant excess because the reaction of ferryl ion with iron(II) ($k = 1.4 \times 10^5$ $M^{-1}s^{-1}$)[50] is not fast enough compared to the reaction between iron(II) and HSO_5^- ($k = 3.7 \times 10^4$ $M^{-1}s^{-1}$) and FeO^{2+} only reacts with water slowly.[50] In addition, at iron(II) excess the dihydroxo dimer of iron(III), $Fe_2(OH)_2^{4+}$, should be a detectable intermediate because it is the immediate product of the reaction of ferryl ion with iron(II)[50] and only dissociates slowly in sulfuric acid, on a multisecond time scale.[43] It is therefore concluded that the following one-electron-transfer steps are the best way to interpret the reaction:

$$Fe^{2+} + HSO_5^- \rightarrow Fe(OH)^{2+} + SO_4^- \qquad v = k_{39}[Fe^{2+}][HSO_5^-] \quad (39)$$

$$Fe(OH)^{2+} + H^+ \rightarrow Fe^{3+} + H_2O \quad (40)$$

(49) Kirkbright, G. F.; West, T. S.; Woodward, C. *Anal. Chim. Acta* **1966**, *36*, 298–303.
(50) Loegager, T.; Holcman, J.; Sehested, K.; Pedersen, T. *Inorg. Chem.* **1992**, *31*, 3623–3529.
(51) Pestovsky, O.; Stoian, S.; Bominaar, E. L.; Shan, X.; Münck, E., Jr.; Bakac, A. *Angew. Chem., Int. Ed.* **2005**, *44*, 6871–6874.

$$Fe^{2+} + SO_4^{\bullet -} \rightarrow Fe^{3+} + SO_4^{2-} \quad (41)$$

Step 39 is rate determining, therefore $k_{27} = k_{39}$. There is no evidence to exclude either inner-sphere or outer-sphere electron transfer for reaction 39. In any case, the cleavage of the peroxo bond in HSO_5^- should be homolytic during the process, and the rate-determining step should be a one-electron oxidation.

A trapping experiment to confirm the participation of $SO_4^{\bullet -}$ was also attempted using Ce(III) (concentrations: 1.0 mM HSO_5^-, 1.0 mM Fe(II), 10 mM Ce(III), 0.10 M H_2SO_4) following a strategy used successfully in an earlier study of the V(IV) system.[18] Spectrophotometric data gave no evidence for any Ce(IV) formation in this experiment. However, this result only indicates that the experiment was inconclusive and provides no evidence against the involvement of $SO_4^{\bullet -}$. A successful trapping experiment (i.e., detection of ceric ion) would require the reaction between Fe(II) and $SO_4^{\bullet -}$ to be not much faster than the reaction between Ce(III) and $SO_4^{\bullet -}$. This criterion might not be fulfilled in the system. In addition, the reaction between Ce(IV) and Fe(II) is quite fast (1.3×10^6 $M^{-1}s^{-1}$)[52] compared to the reaction between Fe(II) and HSO_5^- (3.7×10^4 $M^{-1}s^{-1}$). Even if Ce(IV) is formed in the trapping reaction, Fe(II) would consume it rapidly.

In the earlier report about the reaction of V(IV) with HSO_5^-, the reaction was assumed to comprise a rate-determining one-electron transfer step, and evidence for the involvement of the sulfate ion radical was also obtained by the trapping experiment with Ce(III).[18] This scheme can be extended in a straightforward way to interpret the pH-dependence as well:

$$VO^{2+} + H_2O = VO(OH)^+ + H^+ \qquad K_{42} = \frac{[VO(OH)^+][H^+]}{[VO^{2+}]} \quad (42)$$

$$VO^{2+} + HSO_5^- \rightarrow VO(OH)^{2+} + SO_4^{\bullet -} \qquad v = k_{43}[VO^{2+}][HSO_5^-] \quad (43)$$

$$VO(OH)^+ + HSO_5^- \rightarrow VO_2^+ + SO_4^{\bullet -} + H_2O \qquad v = k_{44}[VO(OH)^+][HSO_5^-] \quad (44)$$

$$VO(OH)^{2+} \rightarrow VO_2^+ + H^+ \quad (45)$$

$$VO^{2+} + SO_4^{\bullet -} \rightarrow VO^{3+} + SO_4^{2-} \quad (46)$$

Again, no distinction between inner- or outer-sphere pathways for reactions 43 and 44 are possible, but the rate-determining step is certainly a one-electron oxidation. Equilibrium 42 is known from the literature.[53] The value of K_{42} (8.5×10^{-7} M) is a lot smaller than the acid concentrations used in this study. Consequently, rate-determining parallel reactions 43 and 44 interpret the k_{20a} and k_{20b} pathways respectively with $k_{20a} = k_{43}$ and $k_{20b} = k_{44}K_{42}$.

As shown by our experiments, Ce(III) is not oxidized directly by HSO_5^-. The reaction between these two reagents can be induced by γ radiation.[54] In this work, it was shown that UV light can also drive the process. A related photoreaction between Ce(III) and $S_2O_8^{2-}$ is also known from the literature.[55]

Because HSO_5^- cannot absorb a significant amount of light in the presence of Ce(III) (spectra in Figure S25 in the Supporting Information), only the absorption of Ce(III) can be responsible for the photoreaction. It should be kept in mind that the fluorescence of Ce(III), unlike in the photoreaction with $S_2O_8^{2-}$,[55] is not quenched by the oxidant. This is an indication that excited *Ce(III) does not react with HSO_5^- directly. A possible reaction sequence interpreting all our findings is given below:

$$*Ce^{3+} \rightarrow Ce^{4+} + e^- \quad (47)$$

$$e^- + H^+ \rightarrow H \quad (48)$$

$$H + HSO_5^- \rightarrow H_2O + SO_4^{\bullet -} \quad (49)$$

$$Ce^{3+} + SO_4^{\bullet -} \rightarrow Ce^{4+} + SO_4^{2-} \quad (50)$$

In this sequence, the absorption process, that is the formation of $*Ce^{3+}$, is rate determining. It should also be noted that reactions 47−49 are known from the literature[56] and reaction 50 has also been proposed to take place in an earlier studies in different systems.[18,31]

Standard redox potentials[57,58] provide further insight into mechanistic aspects of the reactions studied here. The standard potential of HSO_5^-/HSO_4^- is 1.84 V, whereas that of $SO_4^{\bullet -}/HSO_4^-$ is 2.49 V. From these two values, the potential for one-electron reduction of HSO_5^- can be calculated for the redox copule $HSO_5^-/SO_4^{\bullet -}$: 1.19 V. The one-electron oxidation of halides would necessarily involve the formation of halogen atoms, and the redox potentials of the corresponding processes are higher than 1.19 V ($Cl^{\bullet}/Cl^-$ 2.41 V, $Br^{\bullet}/Br^-$ 1.92 V, $I^{\bullet}/I^-$ 1.33 V). Therefore, formation of $SO_4^{\bullet -}$ would be a thermodynamically uphill step in these cases. In the case of chloride ion, this first step would require $(2.41 - 1.19) \times 96.485 = 118$ kJ/mol free energy input. The activation free energy calculated for 298 K based on the data given in Table 2 is only 89 kJ/mol, which excludes the possibility of one-electron oxidation in the case of chloride ion. A similar line of thought does not exclude one-electron oxidation for I^- and Br^-. However, the pH-dependence of the $HSO_5^-/SO_4^{\bullet -}$ potential ($H^+ + HSO_5^- \rightarrow SO_4^{\bullet -} + H_2O$) should also be kept in mind. Figure 2 shows that the kinetics is unchanged as the pH is shifted from 1 to 8. At pH 8, the $HSO_5^-/SO_4^{\bullet -}$ formal potential is $1.19 + 0.0591 \times \lg 10^{-8} = 0.72$ V. The free energies of the possible one-electron steps would thus be $(1.33 - 0.72) \times 96.485 = 59$ kJ/mol for I^- and $(1.92 - 0.72) \times 96.485 = 116$ kJ/mol for Br^-. These are again larger than the corresponding experimental values for the free energies of

(52) Dulz, G.; Sutin, N. *Inorg. Chem.* **1963**, *2*, 917–921.
(53) Nagypál, I.; Fábián, I. *Inorg. Chim. Acta* **1982**, *61*, 109–113.
(54) Matthews, R. W.; Mahlman, H. A.; Sworski, J. T. *J. Phys. Chem.* **1970**, *74*, 2475–2479.
(55) Matthews, R. W.; Sworski, J. T. *J. Phys. Chem.* **1975**, *79*, 681–686.
(56) Shilov, V. P.; Yusov, A. B. *High Energy Chem.* **1999**, *33*, 242–245, and references therein.
(57) Bratsch, S. G. *J. Phys. Chem. Ref. Data* **1989**, *18*, 1–21.
(58) Stanbury, D. M. *Adv. Inorg. Chem.* **1989**, *33*, 69–138.

activation, 55 kJ/mol for I^- and 74 kJ/mol for Br^- at 298 K. Consequently, these thermodynamic arguments rule out an initial one-electron step for every halide ion. The Ce(IV)/Ce(III) redox potential is 1.72 V, it considerably shifts (1.45 V) in 1.0 M sulfuric acid because of complex formation.[59] Neither of these values are low enough to make a direct one-electron reaction between Ce(III) and HSO_5^- likely. However, sulfate ion radical is a strong enough oxidant to oxidize Ce(III) to Ce(IV) as written in eq 50. In the case of Fe(II) and V(IV) (Fe^{3+}/Fe^{2+}, 0.77 V; VO_2^+/VO^{2+}, 1.00 V), the possibility of a one-electron first step is not excluded by thermodynamics. It is also notable that the reaction with the higher driving force (i.e., Fe^{2+}) is faster. Finally, these considerations can also be used to show that the obvious alternative to eq 2 where hydroxyl radical and sulfate ion are the products is quite unlikely to happen:

$$HSO_5^- + e^- \rightarrow SO_4^{2-} + OH \qquad (51)$$

The literature value for the potential $(H^+,OH^{\cdot})/H_2O$ is 2.72 V.[58] This gives 0.96 V for the redox potential of half-reaction 51, which would make HSO_5^- a less-powerful one-electron oxidizing agent, for example it could not oxidize V(IV) in this way.

Further interesting observations can be made by inspecting the activation parameters listed in Table 2.[15,17,18,60−63] It should be noted that very critical reading of the literature is necessary to find sound values of activation parameters. Our overview showed that about half of the reported activation parameters cannot be called reliable or meaningful. There are three recurring errors in determining activation parameters.[64−66] The first is giving activation parameters for nonelementary processes. These values have no diagnostic value in mechanistic studies. The second common error is determining activation parameters without considering the temperature dependences of equilibrium constants used for calculating elementary rate constants. The third common problem is calculating activation parameters based on measurements carried out at two temperatures only. A further misconception is that activation entropies are less reliable than activation enthalpies. In fact, these two parameters are equally reliable provided that the temperature dependencies of the rate constants are correctly evaluated.[67]

The activation parameters in Table 2 characterize the corresponding elementary reaction steps. It is easily noted that all the reactions likely to proceed through an initial two-electron oxidation with heterolytic O−O bond cleavage have activation entropies from −80 to −130 J/mol/K. The two proposed one-electron processes (homolytic O−O bond cleavage) have much smaller activation entropies (−27 and −34 J/mol/K). This is not surprising as the two-electron oxidation is probably an oxygen-atom transfer process in most cases, which is expected to involve much more geometric reorganization than a one-electron rate-determining step, in which only electrons may be transferred before the transition state is reached. Although the number of one-electron oxidation examples is too low for generalization, the data in Table 2 suggest that the activation entropy might be an indicator that helps distinguish between rate-determining one- and two-electron oxidations in the reactions of HSO_5^-.

Conclusions

In this work, it is shown that peroxomonosulfate ion can be involved in both one- and two-electron oxidation in the rate-determining step. The thermodynamics of the formation of the sulfate ion radical is a limiting factor for one-electron processes. Although the use of activation parameters as mechanistic indicators is not without problems in general, present data suggest that the activation entropy may be helpful in this case in distinguishing between the two pathways: $\Delta S^{\ddagger}$ is around −30 J/mol/K for two examples of one-electron reactions of HSO_5^- studied here, whereas about 20 examples show $\Delta S^{\ddagger}$ around −100 J/mol/K for the rate-determining two-electron steps.

Another important point of this work is the production of Cl_2 in the reaction between HSO_5^- and Cl^-. It is the final product at halide excess, whereas a long-lived, high-concentration intermediate at oxidant excess. As avoiding chlorination byproducts is the most important driving force of seeking alternatives to the use of Cl_2 in water treatment, these results show that reaction conditions must be very carefully controlled when Oxone is used.

Acknowledgment. The authors thank the Tempus Foundation and Hungarian Science Foundation (OTKA) for financial support under grant Nos. UT60093/06-07, F049498, and K68668. Mr. Gábor Horváth is acknowledged for help with the spectrofluorometric measurements. G.L. wishes to thank the Hungarian Academy of Sciences for a Bolyai János Research Fellowship. Helpful suggestions from Prof. James H. Mayer and an anonymous reviewer are also gratefully acknowledged.

Supporting Information Available: Concentration dependence plots, ionic strength dependence plot, Eyring plots, and mathematical deductions of various equations. This material is available free of charge via the Internet at http://pubs.acs.org.

IC801569K

(59) Paulenova, A.; Creager, S. E.; Navratil, J. D.; Wei, Y. *J. Power Sources* **2002**, *109*, 431–438.
(60) Betterton, E. A. *Environ. Sci. Technol.* **1992**, *26*, 527–532.
(61) Betterton, E. A.; Hoffman, M. R. *J. Phys. Chem.* **1988**, *92*, 5962–5965.
(62) Thompson, R. C.; Wieland, P.; Appelman, E. H. *Inorg. Chem.* **1979**, *18*, 1974–1977.
(63) Bunton, C. A.; Foroudian, H. J.; Kumar, A. *J. Chem. Soc., Perkin Trans. 2* **1995**, 33–39.
(64) Connick, R. E.; Lee, S.; Adamic, R. *Inorg. Chem.* **1993**, *32*, 565–571.
(65) Betterton, E. A.; Hoffman, M. R. *Environ. Sci. Technol.* **1990**, *24*, 1819–1824.
(66) Johnson, R. W.; Edwards, J. O. *Inorg. Chem.* **1966**, *5*, 2073–2074.
(67) Lente, G.; Fábián, I.; Poe, A. J. *New J. Chem.* **2005**, *29*, 759–760.